Australia: Climate-Ecosystems Variability and Impacts on Disease

K. Cortney Gustafson[1], Mouhamad Diabate[2], Assaf Anyamba[2]

[1] Florida International University, Dept. of Earth and Environment, Miami, FL

[2] USRA-GESTAR & NASA Goddard Space Flight Center, Biospheric Sciences Laboratory, Greenbelt, MD

Introduction

Climate variability in Australia is largely driven by an atmospheric phenomenon called the Southern Oscillation which involved a see-saw like behavior between low and high pressure systems within the equatorial Pacific regions. Due to this phenomenon and its interactions with El Niño, the abnormal warming of sea surface temperatures (SSTs), Australia experiences severe droughts typically during the winter/spring in years when the El- Niño-Southern Oscillation (ENSO) events occur. In contrast, during La Niña events, the abnormal cooling of SSTs, Australia receives unusually high amounts of rainfall and consequential flooding during the winter/spring in years of ENSO events.

Murray Valley Encephalitis (MVE) virus is a rare but fatal mosquito-borne disease which attacks neurological and muscular functioning of humans and animals causing fevers, sometimes progressing to comas, or death. MVE is only transmitted to humans via infected mosquitoes. Therefore, it is assumed that the risk of human infection increases with mosquito populations (Figure 1). Since it is known that mosquitoes breed in vegetated, warm, moist environments, a wet Australian landscape is ideal for mosquito population growth.

This study operates under the theory that increased rainfall, as a result of La Niña events, (a) creates ideal habitats for mosquito population growth and (b) increases vegetation growth, thereby, increasing Normalized Difference Vegetation Index (NDVI) values above normal. Under these premises, positive NVDI anomalies are used as indicators of increased rainfall – associated with ENSO – allowing for a site specific correlation analysis to be done for period of MVE outbreaks. The objective of this research is to show whether the risk of MVE contraction correlates with climate and ecosystem variability via the relationship between rainfall and NDVI anomalies. To do so this research makes use NASA's Terra Moderate Resolution Imaging Spectroradiometer (MODIS) sensor (Figure 2).

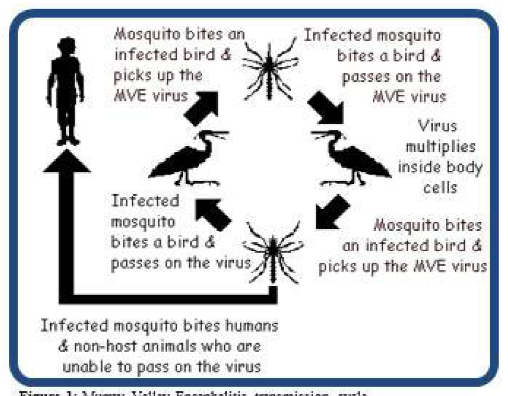

Figure 1: Murray Valley Encephalitis transmission cycle [Source: University of Western Sydney (http://iceh.uws.edu.au/fact_sheets/FS_murray.html)]

Figure 2: NASA's Terra MODIS satellite [Source: NASA Jet Propulsion Laboratory (http://www.nasa.gov/centers/jpl/missions/aster.html)]

Data

1.) Monthly NDVI data were obtain through the follow sources:

- USGS-NASA LP NAAC data pool:
  - Terra MODIS satellite data
  - All MOD13C2 files between January 2000 and May 2012
    - Example data shown in Figures 3 and 4

2.) MVE outbreak data were compiled using the following sources:

- Pro-MED mail database
  - All medical publications, i.e. newspaper and journal articles, of reported MVE infections between March 2009 and September 2011
- Australian Government's Department of Heath
  - National Notifiable Disease Surveillance System (NNDSS) – all confirmed human cases of MVE
    - Table 1 shows collective list

Town	Latitude	Longitude	Date	Effected
2009				
Pilbara	-22.3042	117.9249	6-Mar-2009	Chickens
Kimberley	-41.3986	146.4917	12-Mar-2009	Chickens
Pilbara	-22.3042	117.9249	12-Mar-2009	Chickens
Darwin	-12.4628	130.8418	20-Mar-2009	58-yr old male (died)
Broome	-17.9512	122.2443	1-Mar-2009	2-yr old child (died)
Port Hedland	-20.3116	118.5753	18-May-2009	47-yr old male (died)
Carnarvon	-24.8827	113.6570	18-May-2009	Chickens
Darwin	-12.4628	130.8418	20-May-2009	63-yr old male (died)
2010				
Tennant Creek	-19.6458	134.1912	16-Apr-2010	Chickens
Jabiru	-12.6728	132.8327	16-Apr-2010	Chickens
Borroloola	-16.0880	136.3051	16-Apr-2010	Chickens
2011				
Hawksbury Valley	-33.6096	150.8619	1-Feb-2011	Horse
Upper Hunter Valley	-32.4804	150.7579	1-Feb-2011	Horse
Riverland	-34.4427	140.1833	15-Feb-2011	Horse/45
Port Pirie	-33.1771	138.0101	15-Feb-2011	Horse
Victor Harbor	-35.5532	138.6229	15-Feb-2011	Horse
Mildura	-34.2063	142.1356	23-Feb-2011	Chickens
Robinvale	-34.5843	142.7721	23-Feb-2011	Chickens
Kerang	-35.7340	143.9203	23-Feb-2011	Chickens
Barmah	-36.0174	144.9614	23-Feb-2011	Chickens
Tooleybuc (Swan Hill)	-35.0297	143.3365	23-Feb-2011	Chickens
Sunraysia	-34.2440	142.2762	6-Mar-2011	male (died)
Macquarrie Marshes	-30.4648	147.5103	10-Mar-2011	Chickens
Echuca	-36.8095	144.2224	11-Mar-2011	Horse/1 (died)
Riverland	-34.4427	140.1833	11-Mar-2011	Horse/3
Lower Murray region	-35.0382	141.9803	30-Mar-2011	Birds
Riverland	-34.4427	140.1833	31-Mar-2011	47-yr old male (died)
Riverland	-34.4427	140.1833	31-Mar-2011	27-yr old male (died)
New South Wales	-31.2532	146.9211	31-Mar-2011	Horse/>100
Northern Victoria	-36.3178	144.6854	3-Apr-2011	Horse
Ballarat	-37.5621	143.8561	3-Apr-2011	Horse
South Australia	-30.0002	136.2092	3-Apr-2011	Horse
New South Wales	-31.2532	146.9211	3-Apr-2011	Horse
Victoria	-37.4713	144.7852	7-Apr-2011	Horse
Victoria	-37.4713	144.7852	7-Apr-2011	Horse/18 (died)
Pilbara	-22.3042	117.9249	12-Apr-2011	4-5 suspected human cases
Kimberley	-41.3986	146.4917	12-Apr-2011	4-5 suspected human cases
Carnarvon	-24.8827	113.6570	12-Apr-2011	Male (died)
Darwin	-12.4628	130.8418	13-May-2011	19-yr old female (died)
Alice Springs	-23.7002	133.8806	13-May-2011	19-yr old female (died)
Perth	-31.9529	115.8573	27-May-2011	29-yr old male (died)
Kimberley	-41.3986	146.4917	27-May-2011	2-yr old child (died)

Table 1: Documented MVE outbreaks in Australia from March 2009 – September 2011. Color references for Graphs 1-4: [Yellow] Pilbara region case study sites, [Pink] Hunter, NSW region case study sites, [Orange] Riverland region case study sites, [Purple] Lower Murray region case study sites

Figure 3: MOD13C2 MODIS imaging of global NDVI for June 2006 Source: USGS-NASA LP DAAC data Pool (https://lpdaac.usgs.gov/get_data/data_pool/)

Figure 4: MOD13C2 MODIS imaging of global NDVI for December 2009 Source: USGS-NASA LP DAAC data Pool (https://lpdaac.usgs.gov/get_data/data_pool/)

Methods and Analysis

- **Data Collection:**
  - MVE data were extracted from Pro-Med and National Notifiable Disease Surveillance System (NNDSS)
  - Monthly NDVI data were obtained from USGS-NASA LP NAAC data pool
- **Geo-code and GIS mapping of MVE outbreaks:**
  - Used a latitude/longitude finder website to establish geographical coordinates for each reported incident (http://www.satsig.net/maps/lat-long-finder.htm)
  - Used ArcMap 10 to create GIS maps to represent the spatial and temporal distributions of collected MVE data (Figure 5)
- **Construct IDL code for anomalies:**
  - Wrote IDL code to read a subset monthly time series NDVI data for Australia
  - Wrote code to calculate monthly long-term means and anomalies
  - Mapped selected 2009-2011 monthly anomalies focusing on September – May period when ENSO influence on the climate regime is notable
- **Extracted time series NDVI statistics centered on selected MVE outbreak sites::**
  - Using selected outbreak sites: (1) SE Southern Australia [Riverland]; (2)Hunter, New South Wales [Hawksbury Valley]; (3) Western Australia [Pilbara]; (4)Lower Murray Valley Region, Southern New South Wales [Barmah]
- **Perform statistical analysis :**
  - Using lag analysis between NDVI and timing of MVE outbreaks

Results

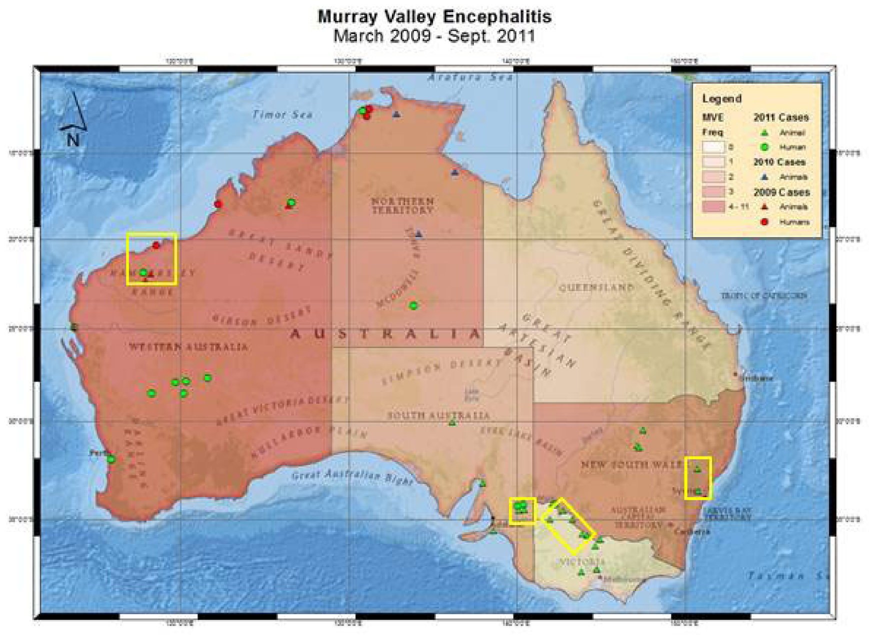

Figure 5: GIS mapping of MVE outbreaks in Australia between March 2009 and September 2011. Green symbols show both human (circles) and animal (triangles) outbreaks in 2011. Blue symbols show only animal outbreaks in 2010 since no human outbreaks were documented for this year. Red symbols show both human (circles) and animal (triangles outbreaks in 2009. Territories are shaded from dark to light showing the higher to lower rates, respectively, of human (only) MVE outbreaks. Some data points are only as accurate to the extent of the spatial scale of specific territories rather than cities/towns due to data collection restrictions: Yellow boxes show regions chosen for time-series plots and lag analyses due to their relatively high MVE activity and known location accuracy. Boxed region from left to right: Pilbara, Riverland, Lower Murray Valley, and Hunter.

NDVI Time Series Plots

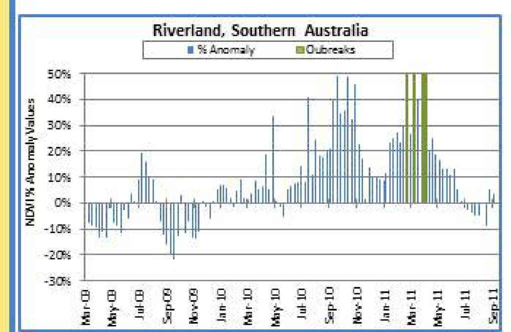

Graph 1: Four outbreaks in the Riverland area of Southern Australia occurred around March 2011 which corresponds with a 20% - 40% increase of NDVI values

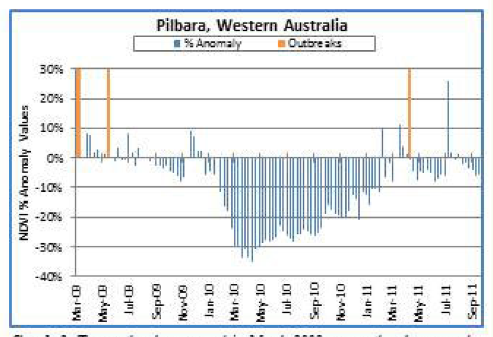

Graph 3: Two outbreaks occurred in March 2009, one outbreak occurred in May 2009 and one outbreak occurred in April 2011 corresponding with 10%, 5% and 5% NDVI increase respectively

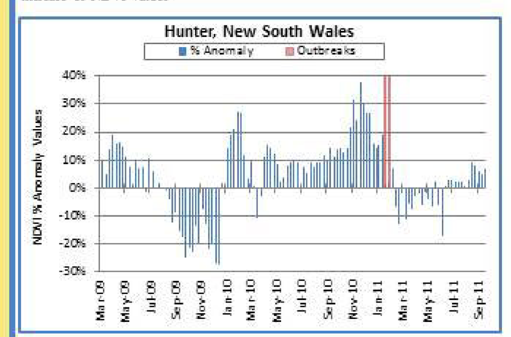

Graph 2: Two outbreaks in the Hunter region of New South Wales occurred in Feb. 2011 following two months of 20%-35% NDVI increase

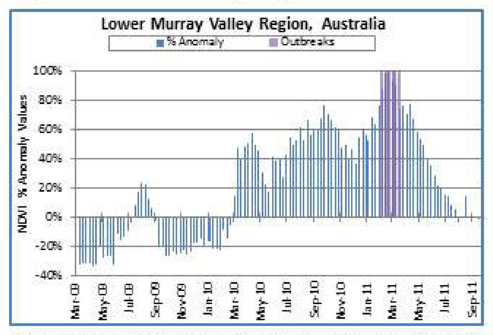

Graph 3: Seven outbreaks in the lower Murray region occurred during March 2011 which corresponds with a 60 -100% NDVI increase

NDVI % Anomaly: March 2009 MVE

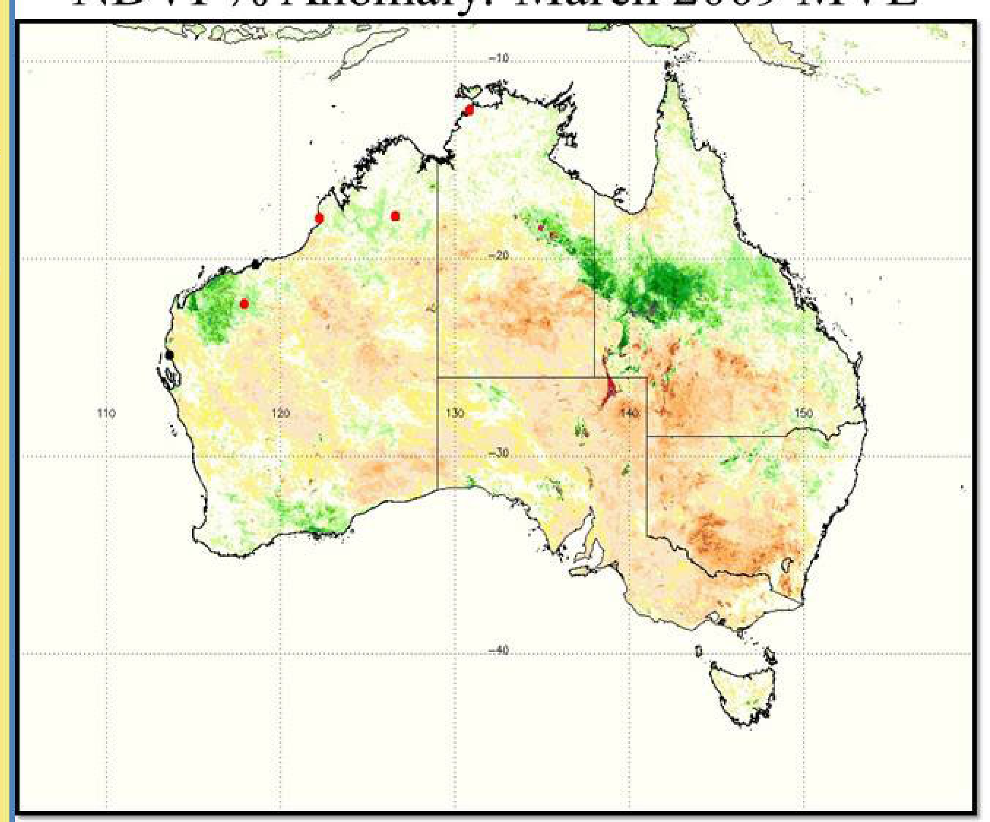

NDVI % Anomaly: March 2011 MVE

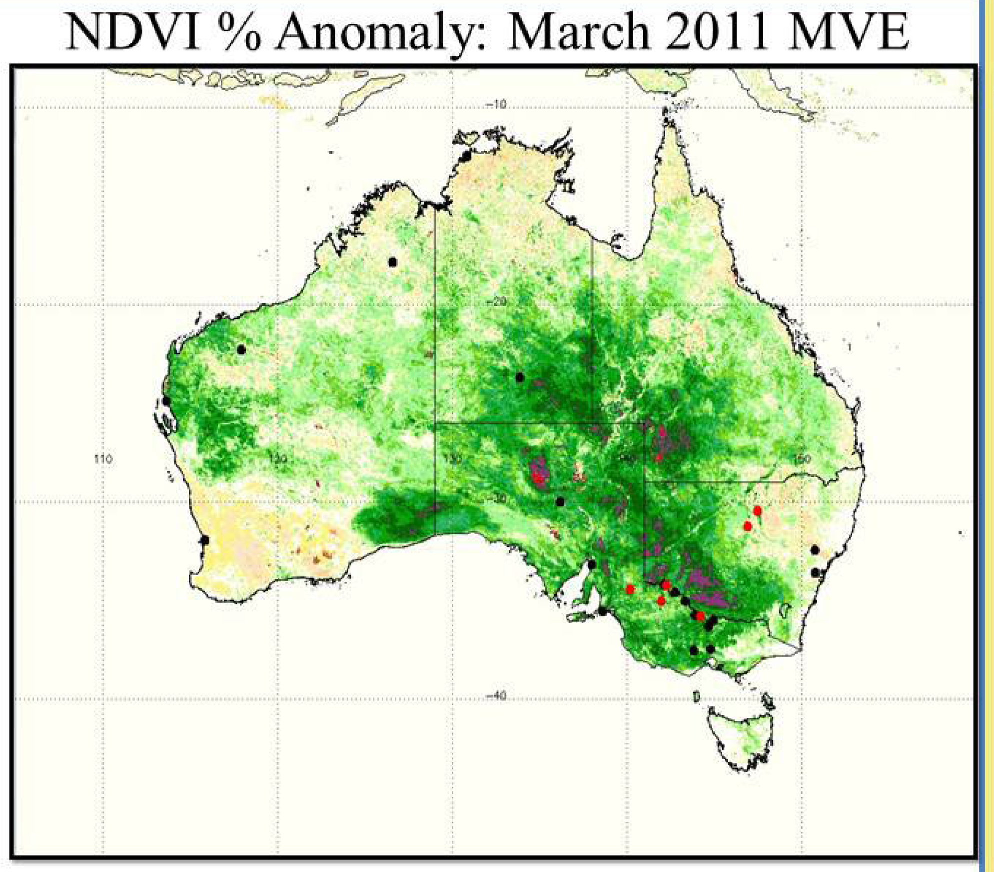

NDVI % Anomaly: April 2010 MVE

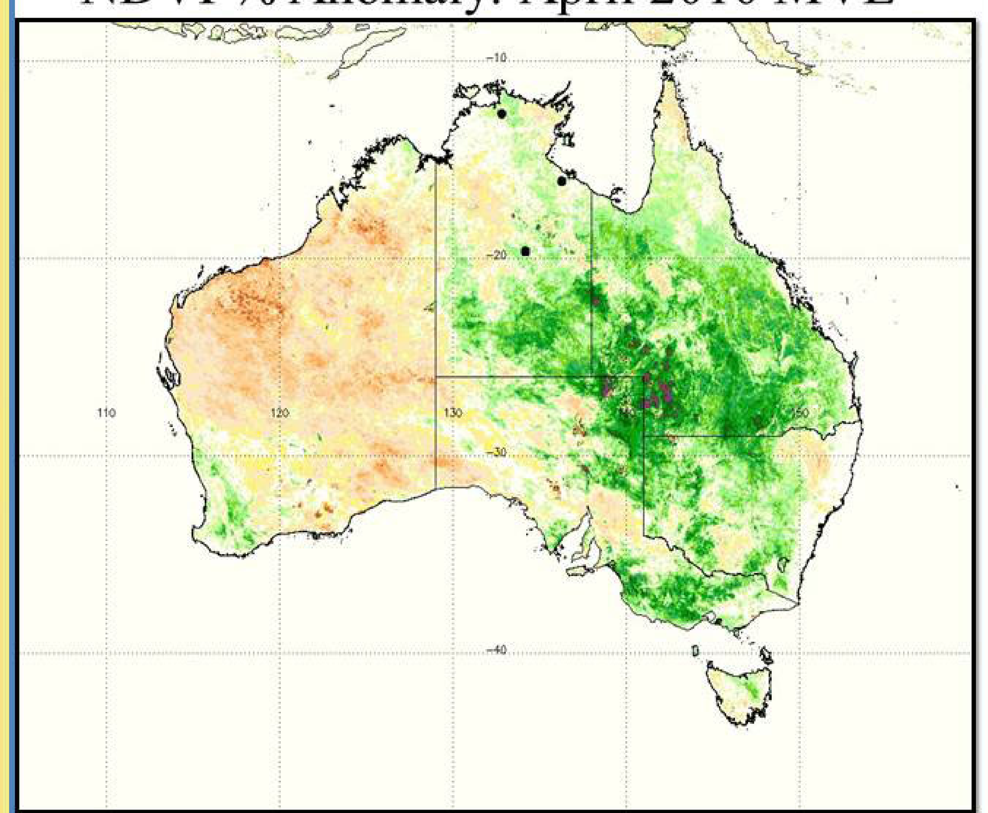

Figures 6-8: [6] Top left – Map of Australia showing NDVI % Anomaly for March 2009, the most active MVE month of given year, and associated points of occurrences; [7] Bottom left – Map of Australia showing NDVI % Anomaly for April 2010, the most active MVE month of given year, and associated points of occurrences; [8] Top right – Map of Australia showing NDVI % Anomaly for March 2011, the most active MVE month of given year, and associated points of occurrence. **Black** points indicate cases which occurred during the selected months. **Red** points indicate cases which occurred during other months of the selected year. The % Anomaly color scale ranges from: **(+high)** Violet– Green – Yellow – Orange – Red (- low)

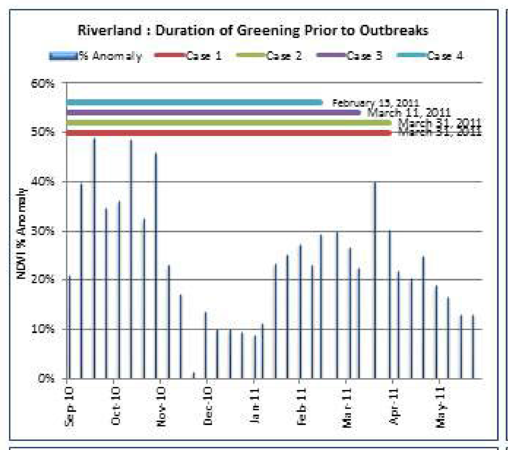

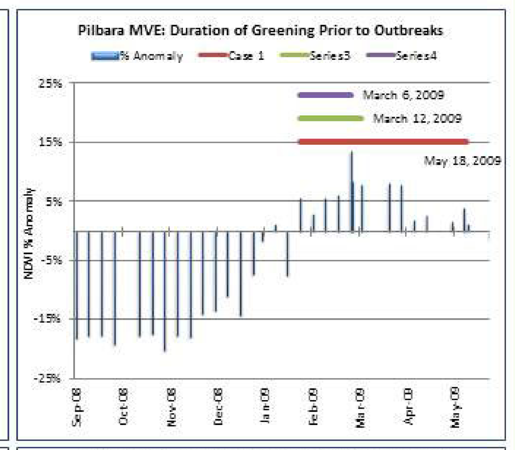

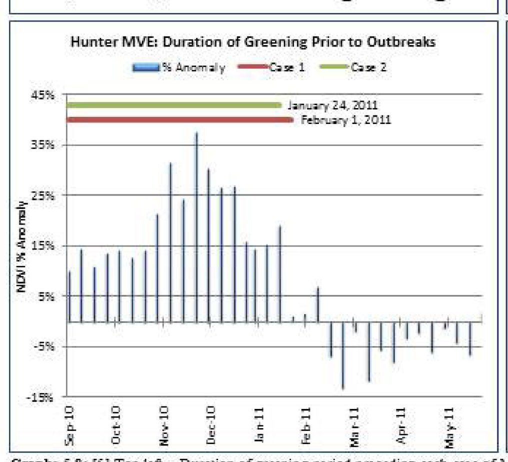

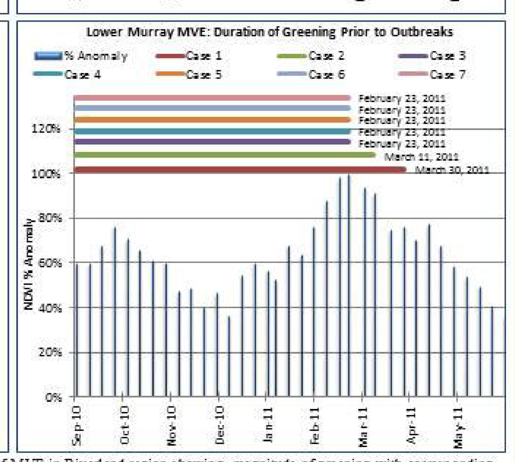

Graphs 5-8: [5] Top left – Duration of greening period preceding each case of MVE in Riverland region showing magnitude of greening with corresponding NDVI % Anomaly; [6] Bottom left - Duration of greening period preceding each case of MVE in Hunter region showing magnitude of greening with corresponding NDVI % Anomaly; [7] Top right - Duration of greening period preceding each case of MVE in Pilbara region showing magnitude of greening with corresponding NDVI % Anomaly; [8] Bottom right - Duration of greening period preceding each case of MVE in Lower Murray region showing magnitude of greening with corresponding NDVI % Anomaly

Results

The most active areas for MVE cases and their respective NDVI % anomaly values were plotted to show the corresponding temporal distribution between the two variables (Graphs 1 – 4). The results show a general lag and positive correlation between increases in NDVI % anomaly and timing of outbreaks (Graphs 5 – 6).

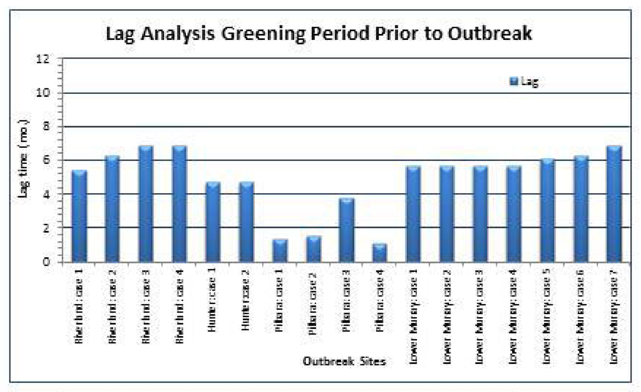

Graph 9: Lag analysis for each case study outbreak occurrence and the duration of previous greening period

The most active months for MVE cases in 2009, 2010 and 2011 were mapped with their associated NDVI % anomaly values (Figures 6 – 8). The results show a general greening trend in the areas of infection indicating a relationship between positive NDVI % anomaly values and the presence MVE.

The four chosen case study sites had greening periods extending from 1.37 – 6.9 months prior to each out break, establishing an average lag time of 4.98 months (Graph 9). These results are consistent with the theory that persistent and above normal NDVI, i.e. greening periods associated with above normal rainfall, create ideal habitats for the production and increase in populations of mosquito vectors that transmit MVE.

Conclusion

This research shows that there is a general temporal and spatial correlation between increased NDVI and the risk of Murray Valley Encephalitis contraction. These result support that hypothesis that, in Australia, anomalous increase NDVI is a proxy for increased rainfall creating ideal habitats for increasing mosquito populations. These results support the hypothesis that ENSO-driven climate and ecosystem variability impact disease outbreak patterns . It is suggested to pursue more accurate georeferenced records of MVE outbreaks for robust statistical analysis.

Future Work

It is hoped that this research will be continued to include rainfall data analysis, since currently NDVI is used as a proxy for rainfall. It is apparent that the link between NDVI increases and decreases should be scientifically proven to correspond with rainfall increases and decreases respectively. Such an analysis is necessary to validate that climate variability, i.e. rainfall, is effecting ecosystems, creating ideal mosquito production habitats.

By using satellite imagery to retrieve rainfall data for Australia between the March '09- September'11 time frame, we will be able to calculate monthly rainfall anomalies to compare the higher than average rainfall and lower than average rainfall with higher and lower NDVI % anomaly value respectively. If this data is shows the suggested direct relationship, that final link will then allow us to justifiably claim that ENSO-driven climate variability does impact human health by influencing the risk of transmitting vector-borne diseases such as Murray Valley Encephalitis. Our team anticipates that the Summer of 2013 will allow for such an opportunity.

References

Allan, R. 2000. ENSO and climate variability in the Past 150 years. In *El Niño and the Southern Oscillation: Multiscale Variability and Global and Regional Impacts,* eds. H.F. Diaz and V. Markgraf, New York, NY: Cambridge University Press.

Anyamba, A. and C. Tucker. 2012. Historical perspectives on AVHRR NDVI and vegetation drought monitoring. In *Remotes Sensing of Drought: Innovative Monitoring Approaches,* eds. B.D. Wardlow, M.A. Anderson, and J.P. Verdin, Boca Raton, FL: CRC Press, in press.

IOM (Institute of Medicine). 2008. *Global Climate Change and Extreme Weather Events: Understanding the Contributions in Infectious Disease Emergence.* Washington, DC: The National Academic Press.

Katz, R. 2002. Sir Gilbert Walker and a connection between El Niño and statistics. *Statistical Science*, 17:1, 97-112.

Nicholls, N. 1991. Teleconnections and health. In *Teleconnections Linking Worldwide Climate Anomalies*, eds. M.H.Glantz, R.W. Katz and N. Nicholls, New York, NY: Cambridge University Press.

Trenberth, K. 1991. General characteristics of El Niño-Southern Oscillation. In *Teleconnections Linking Worldwide Climate Anomalies*, eds. M.H.Glantz, R.W. Katz and N. Nicholls, New York, NY: Cambridge University Press.

Tucker, C.J., 1979. Red and Photographic infrared linear combinations for monitoring vegetation. *Remote Sensing of Environment*, 8, 127 – 150.

Acknowledgements

This research was conducted under the guidance of Dr. Assaf Anyamba, Mouhamad Diabate, and Jennifer Small as part of the Biospheric Sciences Labratory at NASA's Goddard Space Flight Center with additional programming assistance from Matt hew Smith. This research was funded by NASA WaterSCAPES at Florida International University, headed by Dr. Fernando Miralles-Wilhelm.